PHYSICAL REVIEW D **82,** 125038 (2010)

Strange mass dependence of the tricritical point in the $U(3)_L \times U(3)_R$ chiral sigma model

A. Jakovác*
Physics Institute, BME Technical University, H-1111 Budapest, Hungary

Zs. Szép†
Statistical and Biological Physics Research Group of the Hungarian Academy of Sciences, H-1117 Budapest, Hungary
(Received 16 July 2010; published 29 December 2010)

We study the strange quark mass dependence of the tricritical point of the $U(3)_L \times U(3)_R$ linear sigma model in the chiral limit. Assuming that the tricritical point is at a large strange mass value, the strange sector as well as the $\eta - a_0$ sector decouples from the light degrees of freedom which determines the thermodynamics. By tracing this decoupling we arrive from the original $U(3)_L \times U(3)_R$ symmetric model, going through the $U(2)_L \times U(2)_R$ symmetric one, at the $SU(2)_L \times SU(2)_R$ linear sigma model. One-loop level beta functions for the running of the parameters in each of these models and tree-level matching of the coupling of these models performed at intermediate scales are used to determine the influence of the heavy sector on the parameters of the $SU(2)_L \times SU(2)_R$ linear sigma model. By investigating the thermodynamics of this latter model we identified the tricritical surface of the $U(3)_L \times U(3)_R$ linear sigma model in the chiral limit. To apply the results for QCD we used different scenarios for the m_s and μ_q dependence of the effective model parameters, and then the $\mu_q^{\mathrm{TCP}}(m_s)$ function can be determined. Depending on the details, a curve bending upwards or downwards near $\mu_q = 0$ can be obtained, while with explicit chemical potential dependence of the parameters the direction of the curve can change with m_s, too.

DOI: 10.1103/PhysRevD.82.125038 PACS numbers: 11.10.Wx, 11.10.Hi

I. INTRODUCTION

The phase diagram of QCD is a much-studied phenomenon, but still its characteristics, at finite baryon chemical potential, in particular, are far from being settled [1–4]. While at zero chemical potential all the Monte Carlo (MC) and effective model studies tend to support a common picture, at nonzero chemical potential the MC results are inconclusive.

At zero chemical potential the widely accepted phase diagram in the m_{ud}-m_s plane exhibits both at small and at large quark masses regions of first-order phase transition each bounded by a line of second-order critical end points (CEPs). In between these regions, the transition is of the analytic crossover type. If we introduce a nonzero quark baryon chemical potential μ_q, the second-order CEP lines extend to a critical surface. If the critical surface lying closer to the origin of the mass plane bends upwards, that is, to larger quark masses, then there is a possibility that a crossover transition becomes at larger chemical potential a second- and subsequently a first-order phase transition. Direct MC simulations [5,6] and also the estimates in [7,8] give a finite μ_q^{CEP} value, and similar conclusions can be drawn from other lattice techniques, too [9–11]. However, the second-order surface seems to bend downwards, to smaller quark masses, according to studies of the curvature performed on $N_\tau = 4$ lattices for $N_f = 3$ and $N_f = 2 + 1$ cases in [12–16] using imaginary chemical potential. These lattice studies performed at imaginary chemical potential seem to exclude the existence of a CEP for $\mu_q < 166$ MeV even on a finer, $N_t = 6$ lattice used in the $N_f = 3$ case [17], although there the curvature of the critical surface is consistent with zero, but the sign of the curvature is not yet constrained because the cutoff effects appear to be larger than finite density effects. Although all these lattice results do not necessarily contradict each other, they could imply a scenario in which the critical surface has a nontrivial shape. Some numerical evidence for such a possibility is given in [18].

Beyond direct simulations one can approach the study of the phase structure of QCD through effective theories; see e.g. [3,19] for reviews. At finite chemical potential there are several results on the chiral phase transition for two flavors in Nambu–Jona-Lasinio models, as well as in linear sigma models [20–23]. Using the $SU(2)_L \times SU(2)_R$ linear sigma model an interesting phase structure with two CEPs in the $\mu_q - T$ plane was reported for low values of the pion mass in [23]. Considering three flavors, one can study in these models the properties of the chiral critical surface [24–29]. In [24–26] the authors used the $U(3)_L \times U(3)_R$ chiral sigma model near the physical point and found that in the available parameter space the critical surface bends upwards, supporting the direct MC result. In [27–29], in the framework of the extended Nambu–Jona-Lasinio model the authors found a down-bending surface for a small chemical potential which eventually turns back at higher values of μ_q. This behavior would conciliate the two MC scenarios

*jakovac@fizika.phy.bme.hu
†szepzs@achilles.elte.hu

within a single critical surface if the turning happens at positive values of m_{ud} and m_s and finite values of μ_q. Other possible behaviors of the critical surface were discussed in [30,31] using the Gibbs' phase rule for phase coexistence.

In the chiral limit ($m_{ud} = 0$), there are two well-known limits: the $\mu_q = 0$ and the infinite strange quark mass ($m_s = \infty$) limits. At $\mu_q = 0$ we have a first-order phase transition region for small m_s, a second-order transition region at large m_s, and a tricritical point (TCP) separating them, with a characteristic value m_s^{TCP}. At $m_s = \infty$ and small chemical potential we have second order, for large μ_q a first-order phase transition, with again a TCP in between. The line of TCPs is the intercept of the critical surface and the $m_{ud} \equiv 0$ plane of the $m_{ud} - m_s - \mu_q$ space. According to the above scenarios the two TCPs at the $\mu_q = 0$ and $m_s = \infty$ can be connected by a single line with definite curvature, a backbending line, or they may belong to two distinct TCP lines. In the latter case there must be two disjunct critical surfaces in the $m_{ud} - m_s - \mu_q$ space, of which these two TCP lines are just the end points in the $m_{ud} \equiv 0$ plane [30,31].

In this paper we attempt to describe the behavior of the tricritical line in the chiral limit of the $U(3)_L \times U(3)_R$ sigma model [24,32,33], assuming in addition that the mass of the constituent strange quark and the anomaly scale are much larger than the critical temperature. The study of the chiral limit has some advantages, since one can work with much less parameters than in a generic situation. A disadvantage, though, is that in this case there are no direct measurements which could connect the effective model parameters with the QCD (although, strictly speaking, there are no such measurements anywhere, apart from the physical point, especially not for a possible chemical potential dependence of the parameters). The goal of this study is to explore the parameter dependence of the TCP line.

The assumption that the constituent strange mass is much larger than T_c is based on the observation that even at the physical point of the mass plane the constituent strange quark mass is above 450–500 MeV (see Ref. [34] and references therein), while $T_c \sim 160$ MeV, and the critical line in the $m_{ud} - m_s$ plane behaves as $m_s^{\mathrm{TCP}} - m_s \sim m_{ud}^{2/5}$, as one approaches the m_s axis, which predicts for m_s^{TCP} and for the mass of the strange constituent quark a higher value than the corresponding mass at the physical point. Actually, in the lattice study of [35] it was estimated that $m_s^{\mathrm{TCP}} \simeq 2.8 T_c$, while in [33] using the $U(3)_L \times U(3)_R$ sigma model m_s^{TCP} was estimated to be 1 order of magnitude bigger than the value of m_s at the physical point. A similar observation can be made for the anomaly scale, which is connected to the mass of the η' meson. In this physical situation we have a multiscale system, where a simple one-loop analysis would lose the contribution of the heavy sector. Instead, we have to work with decoupling theory [36], which results in a hierarchy of effective models describing the physics at lower and lower scales. First the m_s strange quark sector decouples with the corresponding bosonic degrees of freedom, and we obtain an effective $U(2)_L \times U(2)_R$ symmetric theory. Then the η' sector (which has semilarge masses at $m_s \to \infty$ because of the anomaly) decouples, and we are left with the $SU(2)_L \times SU(2)_R$ chiral sigma model consisting of pion and sigma mesons, as well as the u and d constituent quarks. Here we can use the results of [22] to determine the position of TCP for a given parameter set. The effect of the strange sector on the position of the TCP is only through the modified parameters of the $SU(2)_L \times SU(2)_R$ chiral sigma model. To determine the parameters of the different effective models involved in the analysis we use the one-loop β-function-governed running of these parameters and matching of the corresponding n-point functions in the common validity range of the models. Some extra assumptions on the original parameters of the $U(3)_L \times U(3)_R$ sigma model are unavoidable.

The setup of the paper is as follows. First, we discuss the model in Sec. II. Then, we overview the generic ideas how the decoupling works in Sec. III. Next, we perform the decoupling in the $U(3)_L \times U(3)_R$ model in Sec. IV. We study the thermodynamics in the resulting effective $SU(2)_L \times SU(2)_R$ linear sigma model in Sec. V. We close with conclusions in Sec. VI.

II. THE MODEL

We first construct the starting model [24,32], which is the $U(3)_L \times U(3)_R$ symmetric linear sigma model defined by the Lagrangian:

$$\mathcal{L}_{U(3)} = \bar{\psi}[i\partial - 2gT^a(\sigma_a + i\gamma_5\pi_a)]\psi + \mathrm{Tr}(\partial_\mu\Phi^\dagger\partial_\mu\Phi) - U(\Phi), \tag{1}$$

where T^a are the $U(3)$ generators, $T_a = \lambda_a/2$ for $a = 1, \ldots, 7$, and $T^0 \equiv T^x$, $T^8 \equiv T^y$ [33], with

$$T^x = \frac{1}{2}\begin{pmatrix} 1 & 0 & 0 \\ 0 & 1 & 0 \\ 0 & 0 & 0 \end{pmatrix}, \qquad T^y = \frac{1}{\sqrt{2}}\begin{pmatrix} 0 & 0 & 0 \\ 0 & 0 & 0 \\ 0 & 0 & 1 \end{pmatrix}. \tag{2}$$

The meson matrix $\Phi = \boldsymbol{\sigma} + i\boldsymbol{\pi} = T^a(\sigma_a + i\pi_a)$ is given in terms of the physical degrees of freedom as

$$\boldsymbol{\sigma} = \frac{1}{\sqrt{2}}\begin{pmatrix} \frac{1}{\sqrt{2}}(\sigma_x + a_0^0) & a_0^+ & \kappa^+ \\ a_0^- & \frac{1}{\sqrt{2}}(\sigma_x - a_0^0) & \kappa^0 \\ \kappa^- & \bar{\kappa}^0 & \sigma_y \end{pmatrix},$$
$$\boldsymbol{\pi} = \frac{1}{\sqrt{2}}\begin{pmatrix} \frac{1}{\sqrt{2}}(\eta_x + \pi^0) & \pi^+ & K^+ \\ \pi^- & \frac{1}{\sqrt{2}}(\eta_x - \pi^0) & K^0 \\ K^- & \bar{K}^0 & \eta_y \end{pmatrix}. \tag{3}$$

Finally, the potential for Φ reads

$$U(\Phi) = M^2\,\mathrm{Tr}(\Phi^\dagger\Phi) + \lambda_1[\mathrm{Tr}(\Phi^\dagger\Phi)]^2 + \lambda_2\,\mathrm{Tr}[(\Phi^\dagger\Phi)^2] - \sqrt{2}C(\det\Phi + \det\Phi^\dagger) + \mathrm{Tr}[H(\Phi + \Phi^\dagger)]. \tag{4}$$

Here, C governs the $U(1)$ anomaly which breaks the symmetry to $SU(3)_L \times SU(3)_R$. The last H-dependent term explicitly breaks also this symmetry. As a consequence we consider the case when vacuum expectation values develop for those scalar fields which belong to the center elements of the symmetry group. These are taken into account through the shifts: $\sigma_x \to \sigma_x + x$ and $\sigma_y \to \sigma_y + y$. In this paper we are interested in the regime where the vacuum structure of the theory contains a heavy s-quark sector and a light ud sector, with a corresponding meson sector. For the constituent quark sector this mass hierarchy can be fulfilled with $y \gg x$, since at tree level the s-quark mass is $m_s = \sqrt{2}gy$, while $m_{ud} = gx$. We assume that the mesons containing s quarks have a mass of order m_s, while the rest have a mass of order m_{ud}. No splitting is assumed between u and d quark masses.

After having made all these assumptions, the mass spectrum, and correspondingly the physics, splits into a heavy and a light part. The light sector influences only very little the symmetry breaking pattern of the heavy sector; therefore we may set $x = 0$ when dealing with the determination of the heavy masses. Then we find the following mass relations:

$$\begin{aligned} m_x^2 &= M^2 + \lambda_1 y^2 - Cy, \qquad m_a^2 = M^2 + \lambda_1 y^2 + Cy, \\ m_K^2 &= M^2 + (\lambda_1 + \lambda_2) y^2, \qquad m_y^2 = M^2 + 3(\lambda_1 + \lambda_2) y^2, \\ & m_s^2 = 2g^2 y^2, \end{aligned} \tag{5}$$

where m_x^2 is the mass squared for π_i and σ_x, m_a^2 is the mass squared of η_x and a_i^0, m_K^2 applies for η_y, K, and κ modes, m_y^2 is the mass squared of σ_y, and finally, m_s is the strange quark mass. In the case of a large strange quark mass, i.e. large y values, the lightness of the pion-sigma sector requires that $m_x^2 \ll m_s^2$. This can be achieved only with fine-tuning m^2—after all, this is the manifestation of the hierarchy problem, where the high energy sector influences, through radiative corrections and spontaneous symmetry breaking, the light sector. To circumvent the problem, we parametrize everything with the light x mass:

$$\begin{aligned} m_a^2 &= m_x^2 + 2Cy, \\ m_K^2 &= m_x^2 + \lambda_2 y^2, \\ m_y^2 &= m_x^2 + (2\lambda_1 + 3\lambda_2) y^2. \end{aligned} \tag{6}$$

We see that there is a third mass scale, associated to Cy. Since C has the dimension of a mass, we can relate its value to y or m_x, and it is a matter of the low-lying dynamics determining the details of the effective model to know which is the ''true'' ratio between them. In this work we try to play around with the possible values of C to see its effect on the thermodynamics.

So, after all, we have three possibly very different mass scales: m_s, m_a, and m_x. The thermodynamics of the system, which is related to the spontaneous breaking in the nonstrange sector, must take place at the light scales, that is, at $T \sim m_x$. To treat a physical system with vastly different mass scales is possible only using the fact that for the light physics the heavy degrees of freedom decouple, and their presence can be identified through the values of the parameters of the Lagrangian containing the light degrees of freedom. How this decoupling works in detail is summarized in the next section.

III. DECOUPLING OF MASS SCALES

Here we review the generic principles of decoupling incorporating ideas of heavy mass decoupling (cf. Ref. [36]) and, whenever we switch to a new theory with different degrees of freedom, matching principles (cf. Ref. [37]).

Let us start with a theory with Lagrangian $\mathcal{L}$, coupling constant set $\{g_i\}_{i=1\ldots u}$ (this includes also the masses), and field contents generically denoted with Φ and φ. Let us assume that Φ is much heavier than φ, and their masses are denoted by M and m, respectively.[1] Then we want to establish an effective theory based exclusively on the light degrees of freedom. Let us denote the Lagrangian of this effective theory by $\hat{\mathcal{L}}$, its couplings are $\{\hat{g}_i\}_{i=1\ldots\hat{u}}$ ($\hat{u} \leq u$), and the field content is $\hat{\varphi}$ with mass $\hat{m} \sim m$. We emphasize that, although $\hat{\varphi}$ corresponds to the light degrees of freedom φ of the complete theory, they can differ by wave function renormalization. In general the wave function renormalization and the renormalized couplings of the effective theory depend on the coupling constants of the original theory:

$$\hat{\varphi} = z^{1/2}(g)\varphi, \qquad \hat{g}_i = f_i(g). \tag{7}$$

If we assume that the couplings of the effective model at tree level are linear combinations of the original couplings, then we can write

$$\hat{g}_i = \sum_{j=1}^{u} \mathcal{G}_{ij} g_j + \Delta g_i(g), \qquad i \in [i \ldots \hat{u}], \tag{8}$$

where $\Delta g_i(g)$ denotes the loop corrections which depend on all of the original couplings.

In order to determine these relations we use matching. We take $\hat{u} + 1$ correlators of the light fields at some external momentum and require that their physical value be the same in the original and in the effective model. If we denote the n-point functions of the original and effective model by

$$\begin{aligned} G^n(x_1, \ldots x_n) &= \langle \mathrm{T}\varphi(x_1) \ldots \varphi(x_n) \rangle, \\ \hat{G}^n(x_1, \ldots x_n) &= \langle \mathrm{T}\hat{\varphi}(x_1) \ldots \hat{\varphi}(x_n) \rangle, \end{aligned} \tag{9}$$

then we require in Fourier space

[1] For the sake of simplicity we only consider one heavy and one light degree of freedom.

$$\hat{G}^n(k_1, \ldots k_n) = z^{n/2} G^n(k_1, \ldots k_n) \tag{10}$$

for fixed $k_1, \ldots k_n$. The right-hand side contains, as radiative corrections, the effect of heavy modes.

In perturbation theory the n-point functions depend also on the renormalization scales μ and $\hat{\mu}$, respectively. In general, we expect to obtain all types of logarithmic corrections $\ln^a \mu/E$, where E is any energy scale which shows up in the given n-point function. In loop integrals we typically find $E^2 \sim \max(k_i^2, \text{mass}^2)$, where the mass can be m and M on the right- or $\hat{m}$ on the left-hand side. In order not to have multiple mass scales in the n-point functions (which would lead to large logarithms) we shall choose $|k_i| \sim M$, and then all scales are of the order of M. This means that for the best convergence of the perturbative series we shall also choose $\mu, \hat{\mu} \sim M$. In consequence the relation (7) is in fact established at scale M:

$$\hat{g}_i(M) = \sum_{j=1}^{u} \mathcal{G}_{ij} g_j(M) + \Delta g_i(g(M)). \tag{11}$$

In the original theory the couplings may be defined on a different energy scale M_0. Then, we have to run the couplings according to $\mathcal{L}$ in order to find $g_i(M)$ which is needed above. On the other hand, (11) *defines* $\hat{g}_i$ on the scale M. If we need them on a lower energy scale M', then we have to run them according to $\hat{\mathcal{L}}$, the effective model Lagrangian.

If there are multiple scales to decouple, we have a series of effective models $\mathcal{L}^{(a)}$ with coupling constants $\{g_i^{(a)}\}_{i=1\ldots u_a}$ where the heaviest field has a mass $M_{(a)}$. Then the matching conditions described above lead to the series of equations

$$g_i^{(a+1)}(M_{(a)}) = \sum_{j=1}^{u_a} \mathcal{G}_{ij} g_i^{(a)}(M_{(a)}) + \Delta g_i^{(a)}(g(M_{(a)})). \tag{12}$$

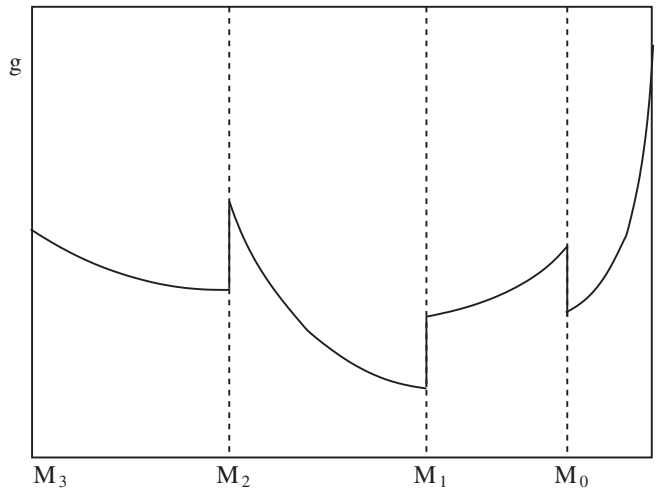

FIG. 1. Schematic plot of the running of a coupling constant. The running between $M_{(a)}$ and $M_{(a+1)}$ is governed by $\mathcal{L}_{(a+1)}$.

This defines the new couplings $g_i^{(a+1)}$ at the mass scale $M_{(a)}$ which, from the point of view of the $a+1$th effective model, is a high energy scale. Then the running of the couplings between $M_{(a)} \to M_{(a+1)}$ is governed by the Lagrangian $\mathcal{L}^{(a+1)}$. This process leads to the schematic running depicted in Fig. 1.

In the most simple version we use tree-level matching, which means that we neglect the Δg_i terms. We use this approximation throughout this work. Moreover, we use the lowest-order (one-loop) beta functions for running.

We start with the $U(3)_L \times U(3)_R$ symmetric linear sigma model which is parametrized at the heavy, strange mass scale in order to avoid the need for running. After the decoupling of the strange sector we are left with a $U(2)_L \times U(2)_R$ model, starting at m_s scale. The beta functions of this model determine the running of the coupling down to m_a, when we switch to $SU(2)_L \times SU(2)_R$ model containing only the σ and π mesons and the u and d constituent quarks. We perform in this model the running of their couplings from m_a down to the T scale, where the finite temperature study is performed.

A separate treatment is needed when we treat the light masses of the system. On one hand, due to the renormalization group (RG) running, they acquire logarithmic dependence on the heavy scale. On the other hand, because of the hierarchy problem discussed in the previous section, the light mass squared m^2 has to be fine-tuned by M^2 in order to keep the light sector truly light. Therefore in bosonic models the logarithmic corrections from the RG running are subleading, and so they should be neglected.

IV. DECOUPLING OF THE HEAVY SECTOR

We use (1) with a background y taken into account via the shift $\sigma_y \to \sigma_y + y$. The first step is to parametrize the heavy sector by determining the parameters of the model at scale m_s. Then, as a next step, we perform the decoupling of the heavy (strange) sector.

A. Parametrization of the heavy sector

We should fix the parameters of the heavy sector by measurements, but there exist no direct mass measurements in this regime. Therefore we are forced to make some assumptions. Since we are in a large quark mass regime, we cannot use the results of the chiral perturbation theory. Instead, the heavy constituent quark model approach, where the masses of the heavy particles are simply the sum of the constituent quark masses, seems to be more adequate. In case of the light-heavy mesons this works nicely, since we can require

$$m_K = m_s \Rightarrow \lambda_2 = 2g^2. \tag{13}$$

In the doubly heavy sector there is a mismatch between the scalar (σ_y) and pseudoscalar (η_y) meson masses, although the constituent quark model would give the same mass for

both. The reason in this model is that there is a symmetry breaking effect in addition to the constituent quark masses. To treat this situation we introduce a free parameter $\bar{\mathcal{A}}$ and require that some average of the two masses squared is $(2m_s)^2$:

$$\bar{\mathcal{A}} m_y^2 + (1 - \bar{\mathcal{A}}) m_K^2 = (2m_s)^2, \tag{14}$$

which results in a relation between the two quartic coupling constants λ_1 and λ_2:

$$\lambda_1 = \left(\frac{3}{2\bar{\mathcal{A}}} - 1\right)\lambda_2. \tag{15}$$

If $\bar{\mathcal{A}} = 1$, i.e. when $m_y = 2m_s$, $\lambda_1 = g^2$ is the smallest value for λ_1. Another plausible choice is $\bar{\mathcal{A}} = 1/2$; then $\lambda_1 = 2\lambda_2 = 4g^2$. Therefore, introducing $\mathcal{A} = -2 + 3/\bar{\mathcal{A}}$ we may set

$$\lambda_1 = \mathcal{A} g^2, \quad \text{where } \mathcal{A} \in [1, \infty]. \tag{16}$$

The parameter range $\mathcal{A} \in [1, 4]$ will be used later in the analysis.

For fixing the other parameters we will use the infrared (IR) sector. We will determine m_σ at its own scale, and this will give the mass unit in the study. For fixing the m_s value at $\mu = m_s$ scale we also use an IR observable. This will be that $m_s^{(0)}$ value where we have a TCP at *zero chemical potential* (but, of course, at finite temperature). Through the decoupling equations this value will determine the original, zero temperature strange quark mass.

B. Tree-level decoupling

The next step is to eliminate the strange sector and determine the parameters of the resulting effective model. The effective model will contain the following degrees of freedom: the upper two (u, d) components in ψ, denoted by ψ_2, and the upper left 2×2 submatrix in Φ, denoted by Φ_2 and containing the $\sigma \equiv \sigma_x$, a_0, η_x, and π fields:

$$\psi = \begin{pmatrix} \psi_2 \\ s \end{pmatrix},$$
$$\Phi = \begin{pmatrix} \Phi_2 & \frac{1}{\sqrt{2}} \boldsymbol{K}_+ \\ \frac{1}{\sqrt{2}} \boldsymbol{K}_-^\dagger & \frac{1}{\sqrt{2}}(\sigma_y + i\eta_y) \end{pmatrix}, \tag{17}$$
$$\boldsymbol{K}_\pm = \boldsymbol{\kappa} \pm i\boldsymbol{K} = \begin{pmatrix} \kappa^+ \pm iK^+ \\ \kappa^0 \pm iK^0 \end{pmatrix}.$$

We split the Lagrangian (1)–(4) according to this characterization of degrees of freedom. The shifted Lagrangian reads

$$\mathcal{L}_{U(3)} = \mathcal{L}_{U(2)} + \mathcal{L}_{\text{heavy}} + \text{const.} \tag{18}$$

Here, $\mathcal{L}_{\text{heavy}}$ contains the heavy part, the "const" term refers to the y-dependent part of the potential, while $\mathcal{L}_{U(2)}$ contains the terms which consist of the light fields:

$$\begin{aligned}\mathcal{L}_{U(2)} = {} & \bar{\psi}_2[i\partial - g\tau_i(\sigma_{2i} + i\gamma_5\pi_{2i})]\psi_2 + \mathrm{Tr}(\partial_\mu \Phi_2^\dagger \partial_\mu \Phi_2) \\ & - (M^2 + \lambda_1 y^2)\,\mathrm{Tr}[\Phi_2^\dagger \Phi_2] - \lambda_1[\mathrm{Tr}(\Phi_2^\dagger \Phi_2)]^2 \\ & - \lambda_2\,\mathrm{Tr}[(\Phi_2^\dagger \Phi_2)^2] + Cy[\det\Phi_2 + \det\Phi_2^\dagger].\end{aligned} \tag{19}$$

Tree-level matching means that we simply neglect the heavy part and go on with the Lagrangian described above. We can argue for this simple choice as follows. The parametrization of the heavy sector of the model could be done only very heuristically, in which case only the leading-order effects could be taken into account. Therefore, it would be inconsistent to work with a detailed decoupling scheme, determining $\Delta g \sim \mathcal{O}(g^2)$ or $\mathcal{O}(g^3)$ corrections to the tree-level values which are not known precisely. For this reason the leading-order approach is the most consistent here. As a result of this approximation we shall trust only the most robust consequences of this study.

C. Running in the $U(2)_L \times U(2)_R$ linear sigma model

In component fields (19) can be written as

$$\begin{aligned}\mathcal{L}_{U(2)} = {} & \bar{\psi}_2[i\partial - g(\varphi_5 - i\gamma_5 a_5)]\psi_2 + \frac{1}{2}(\partial_\mu \varphi)^2 - \frac{m_\varphi^2}{2}\varphi^2 \\ & + \frac{1}{2}(\partial_\mu a)^2 - \frac{m_a^2}{2}a^2 - \frac{\lambda}{4}(\varphi^2 + a^2)^2 \\ & - \frac{\lambda_2}{2}(\varphi^2 a^2 - (\varphi a)^2),\end{aligned} \tag{20}$$

where we introduced the following notations: $\varphi_5 = \sigma_0 + \tau_i\sigma_i$, $a_5 = -\pi_0 - \tau_i\pi_i$, with τ_i being the Pauli matrices, $\lambda = \lambda_1 + \lambda_2/2$, $\varphi = (\sigma, \pi_i)$, and $a = (-\eta, a_i)$. The squared masses are $m_{\varphi/a}^2 = m^2 \mp c$, where $m^2 = M^2 + \lambda_1 y^2$ and $c = Cy$ [cf. (5)].

The running of the couplings are determined by the beta functions given in Appendix A, under Eq. (A32). By solving (A32a) the running of g can be obtained explicitly:

$$g^2(\mu) = \frac{g^2(\mu_0)}{1 - \frac{5g^2(\mu_0)}{12\pi^2}\ln\frac{\mu^2}{\mu_0^2}} = \frac{12\pi^2}{5\ln\frac{\bar{\Lambda}_0^2}{\mu^2}}, \tag{21}$$

where $\bar{\Lambda}_0^2 = \mu_0^2 \exp[12\pi^2/(5g^2(\mu_0))]$. This has an UV Landau pole, while it goes to zero when $\mu \to 0$.

For the other two equations, (A32b) and (A32c), we introduce the ratios

$$u = \frac{2\lambda}{g^2}, \qquad u_2 = \frac{\lambda_2}{g^2}, \tag{22}$$

and a new function $X(\mu)$ monotonous in μ which satisfies

$$\frac{1}{g^2}\frac{dX}{d\ln\mu} = \frac{1}{4\pi^2}. \tag{23}$$

Using (21), this equation has the solution

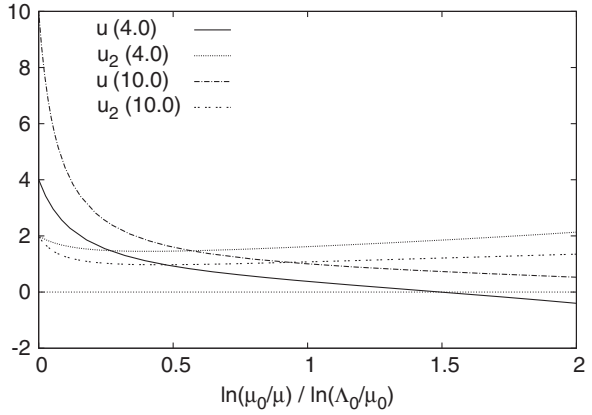

FIG. 2. Running of the ratios $u = 2\lambda/g^2$ and $u_2 = \lambda_2/g^2$ starting from different initial conditions.

$$X(\mu) = \frac{3}{10}\ln\left[\frac{\ln(\bar{\Lambda}_0/\mu_0)}{\ln(\bar{\Lambda}_0/\mu)}\right],$$
$$\ln\frac{\mu_0}{\mu} = \ln\frac{\bar{\Lambda}_0}{\mu_0}(e^{-(10/3)X} - 1) = \ln\frac{\bar{\Lambda}_0}{\mu}(1 - e^{10/3X}). \tag{24}$$

Here we have chosen the condition $X(\mu_0) = 0$, where μ_0 is chosen to be the strange quark mass m_s. Then we find

$$\frac{\partial u}{\partial X} = 4u^2 + 3uu_2 + 3u_2 - 4 - \frac{14}{3}u,$$
$$\frac{\partial u_2}{\partial X} = 3uu_2 + u_2^2 - 4 - \frac{14}{3}u_2. \tag{25}$$

Conforming to Sec. IVA, the phenomenologically motivated initial conditions are $u_2 = 2$ and $u = 2(\mathcal{A} + 1) = 4 \ldots 10$, at the scale of the s quark. The solution of (25) is depicted in Fig. 2. As this plot also demonstrates, for a wide range of μ, u_2 stays in the interval $[1, 2]$, while u decreases continuously as we lower the scale μ from $\mu_0 = m_s$ down to $\mu < m_s$. Sooner or later (depending the initial conditions) u crosses zero which signals the instability of the theory. Probably it means that in order to maintain stability higher-order corrections are needed.

D. Running in the $SU(2)_L \times SU(2)_R$ linear sigma model

If we are well below the m_a scale, then we can use the model containing the $\sigma - \pi$ sector of (20) and the u, d constituent quarks. This model is the $SU(2)_L \times SU(2)_R$ linear sigma model defined by

$$\mathcal{L}_{SU(2)} = \bar{\psi}_2[i\partial\!\!\!/ - g(\sigma + i\gamma_5\tau_i\pi_i)]\psi_2 + \frac{1}{2}(\partial_\mu\varphi)^2 - \frac{m_\varphi^2}{2}\varphi^2 - \frac{\lambda}{4}\varphi^4, \tag{26}$$

where ψ_2 and m_φ^2 were defined in the previous two subsections. The parameters of the model are defined at scale m_a, so we have to apply renormalization group running to find the values of the coupling at the phase transition temperature $T \sim m_\sigma$.

The RG equation is determined in Appendix B, Eq. (B14). The running of g can be solved:

$$g^2(\mu) = \frac{g^2(\mu_0)}{1 + \frac{5g^2(\mu_0)}{24\pi^2}\ln\frac{\mu^2}{\mu_0^2}} = \frac{24\pi^2}{5\ln\frac{\mu^2}{\Lambda_0^2}}, \tag{27}$$

where $\Lambda_0^2 = \mu_0^2\exp[-24\pi^2/(5g^2(\mu_0))]$. This has an IR Landau pole, while it goes to zero when $\mu \to \infty$. The definition of Λ_0 is RG invariant. Comparing (27) with (21), and taking into account that the change of scaling is at $\mu_0 = m_a$, we find

$$\bar{\Lambda}_0^2 = \frac{m_a^3}{\Lambda_0}. \tag{28}$$

For the running of λ we introduce again $X(\mu)$ defined in (23) where now g is the coupling of the $SU(2)_L \times SU(2)_R$ linear sigma model. Using (27) we obtain

$$X(\mu) = \frac{3}{5}\ln\left[\frac{\ln(\mu/\Lambda_0)}{\ln(\mu_0/\Lambda_0)}\right], \qquad \ln\frac{\mu_0}{\mu} = \ln\frac{\mu_0}{\Lambda_0}(1 - e^{5/3X}). \tag{29}$$

We introduce the same ratio as in (22): $2\lambda = ug^2$, and find

$$\frac{du}{dX} = 3u^2 + u - 4. \tag{30}$$

The solution of this equation reads

$$\frac{u-1}{3u+4} = \frac{u_0 - 1}{3u_0 + 4}\left(1 - \frac{\ln(\mu_0/\mu)}{\ln(\mu_0/\Lambda_0)}\right)^{21/5}. \tag{31}$$

This equation has a fixed point at $u = 1$, as is shown in Fig. 3

In the $SU(2)_L \times SU(2)_R$ linear sigma model we can follow the running of the light mass, using (B14). The same running is true for the tree-level sigma mass $m_\sigma^2 \equiv -2m_\varphi^2$. Then we find

$$m_\sigma^2(\mu) = m_\sigma^2(\mu_0)\exp\left[\frac{1}{12\pi^2}\int_0^{\ln\mu/\mu_0} d(\ln(\mu'/\mu_0))g^2(\mu') \times \left(\frac{9}{2}u(\mu') - 1\right)\right]. \tag{32}$$

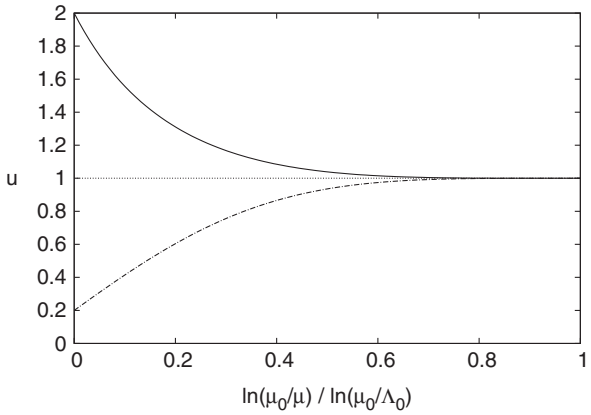

FIG. 3. Running in the $SU(2)_L \times SU(2)_R$ linear sigma model starting from different initial conditions, showing the presence of a fix point at $u = 1$.

With the help of (27) and (31) we obtain

$$m_\sigma^2(\mu) = m_\sigma^2(\mu_0)\exp\left[\frac{7g^2(\mu_0)}{24\pi^2}\int_0^{\ln\mu/\mu_0}\frac{ds}{1+bg^2(\mu_0)s}\times\frac{1+6Y_0z(s)}{1-3Y_0z(s)}\right], \tag{33}$$

where $z(s) = (1+\frac{s}{\ln(\mu_0/\Lambda_0)})^{21/5}$, $b = 5/(12\pi^2)$, and $Y_0 = (u(\mu_0)-1)/(3u(\mu_0)+4)$.

V. THERMODYNAMICS OF THE TRICRITICAL POINT

The one-loop study of the tricritical point in the $SU(2)_L \times SU(2)_R$ linear sigma model was done in [22] using an expansion in the number of flavors. We quote below Eqs. (12) and (14) of that work which determine the position of the tricritical point in the $\mu_q - T$ plane. Using the present notation for the couplings these equations read

$$m_\varphi^2 + T^2\left[\frac{\lambda}{3} + g^2 + \frac{3g^2}{\pi^2}\alpha^2\right] = 0,$$
$$\lambda + \frac{3g^4}{\pi^2}[\ln(\beta\mu) - \mathcal{F}(\alpha)] = 0, \tag{34}$$

where $\beta = 1/T$ is the inverse temperature and $\alpha = \beta\mu_q$ with μ_q the quark baryon chemical potential. The function $\mathcal{F}$ reads

$$\mathcal{F}(\alpha) = 1 - \gamma_E + \ln 2 - \frac{\partial}{\partial s}[\mathrm{Li}_s(-e^\alpha) + \mathrm{Li}_s(-e^{-\alpha})]|_{s=0}. \tag{35}$$

This is a monotonously increasing function of its argument and $\mathcal{F}(0) = 1.5675$.

We choose the scale $\mu = e^\xi T$, where ξ is a number of $\mathcal{O}(1)$. Then the logarithm yields ξ, which effectively modifies $\mathcal{F} \to \bar{\mathcal{F}} = \mathcal{F} - \xi$. In the case of spontaneous symmetry breaking $m_\varphi^2 < 0$, and it is useful to rescale all the masses with the tree-level sigma mass $m_\sigma^2 = -2m_\varphi^2$ at scale μ. Then the equations to solve will be

$$\frac{1}{2} = T^2g^2(\mu)\left[\frac{u(\mu)}{6} + 1 + \frac{3}{\pi^2}\alpha^2\right],$$
$$u(\mu) = \frac{6}{\pi^2}g^2(\mu)\bar{\mathcal{F}}(\alpha). \tag{36}$$

In the complete problem therefore there are $5+2$ parameters. At the UV scale m_s we have m_s, m_a, g^2, u, and u_2, and also we have μ and T at the IR scale. The light mass m_φ or the corresponding m_σ is used as a mass unit. At the TCP $\alpha = \beta\mu_q$ and T can be determined as functions of the UV parameters:

$$\mathcal{G}_0\colon m_s, m_a, g^2, u, u_2 \mapsto \alpha_c, T_c. \tag{37}$$

The final output of the investigation should be, of course, $\alpha_c(m_s)$ and $T_c(m_s)$. But as we just have seen, even in the chiral limit of $m_{ud} = 0$ the problem is five-dimensional instead of one-dimensional. For a sensible prediction we have to say something about the strange mass dependence of m_a, g^2, u, and u_2—these functions should come from the underlying theory, now QCD. Since we do not have this information, we have to assume something sensible.

In the light of the previous subsections we make some approximations. We can fix $u_2(m_s) = 2$, and for u we consider two cases: $u(m_s) = 4$ and $u(m_s) = 10$. The remaining function

$$\mathcal{G}\colon m_s, m_a, g^2 \mapsto \alpha_c, T_c \tag{38}$$

can be plotted as shown in Fig. 4. The detailed numerical strategy to solve the system and obtain this plot is given in Appendix C. Figure 4 shows surfaces in the m_s, m_a, and g^2 parameter space leading to some fixed value of α_c. The $\mu_q/T = 0$ critical surface is a limiting one, in the sense that surfaces with $\mu_q/T > 0$ all lie on one of its sides; they never cross each other. Moreover the normal vector of the surface pointing to positive μ_q/T always has *negative* m_s component—in this sense we can say that going on the direction of the largest μ_q/T change, the surfaces bend downwards in m_s.

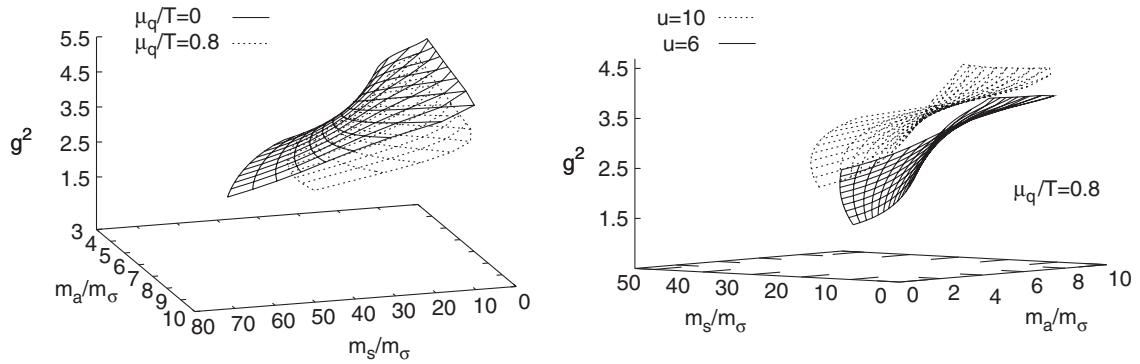

FIG. 4. The dependence of α_c (μ_q/T at the TCP) on the parameters for $u_2(m_s) = 2$. The left panel is obtained with $u(m_s) = 10$. The value of Λ_0 is fixed along the lines of the surfaces directed towards the origin of the $m_s - m_a$ plane. For further information see the main text.

In order to show that different values of u do not change qualitatively the result we plot the $\mu_q/T = 0.8$ surface obtained using $u(m_s) = 10$ and $u(m_s) = 6$ and rescale the g^2 values of the latter by a factor of 1.5. The two surfaces can be seen in the right panel of Fig. 4. As the plot shows, the surfaces have the same characteristics.

Implication of the results for QCD

In real QCD we cannot change m_a, m_s, and g^2 independently. If we knew the m_s dependence of m_a and g^2, then we would have a curve in the $m_s - m_a - g^2$ space parametrized by m_s. This line would go through the critical surfaces characterized by fix μ_q/T, and then we could determine the $m_s(\mu_q/T)$ function. Since we do not have any information on the m_s dependence of the parameters, we explore several possibilities by fixing the value of one of the parameters.

For a constant value of g^2 the m_s dependence of the critical μ_q/T is shown in Fig. 5. One can see that the behavior of this curve depends strongly on how m_a depends on m_s. Characterized by dm_a/dm_s at $\mu_q = 0$, there is a limiting value, and tricritical curves with smaller value of dm_a/dm_s bend downwards (negative curvature); for larger values they bend upwards (positive curvature).

The standard characterization of the behavior of $m_s(\mu_q)$ near $\mu_q = 0$ is through the Taylor series [1]:

$$\frac{m_s(\mu_q)}{m_s(0)} = 1 + \sum_{k=1} c_k \left(\frac{\mu_q}{\pi T}\right)^{2k}. \tag{39}$$

The first two nontrivial terms c_2 and c_4 are shown in Fig. 5 in the case of a constant g^2. The singularity corresponds to that value of the m_s for which the curvature changes sign. It is remarkable that by changing continuously from negative to positive curvatures (c_2 values) we have to go through a singularity.

To have a hint on which curve could be the physical one we recall that the anomaly is mainly a gauge effect, connected to the presence of the instantons [38,39]. This suggests that the dependence of m_a on m_s should be quite small, so the physical line is near to $dm_a/dm_s = 0$. Note that all tricritical surfaces in this model with $m_a =$ constant bend *downwards*.

We see from Fig. 5 that for a wide range of parameter space the c_2 and c_4 are roughly correlated with $c_4 \approx 10c_2$ if $c_2 < 0$ and $c_4 \approx 20c_2$ if $c_2 > 0$. In the rest of the cases c_2 has a large negative value, in which case c_4 is positive. This qualitative behavior can be compared with the results of the numerical simulations. In [12] the authors found $c_2 = -3.3(3)$ and $c_4 = -47(20)$ with $N_f = 3$ degenerate quarks, which seems to be in the first regime. In [16] with $n_f = 2 + 1$ the coefficient c_2 decreased to -39 which means that the results are off the above scaling regime, and we expect a large positive c_4 coefficient—from the behavior of B_4 in the given work $c_4 \approx 10\,000$ with large error bars. Closer to the continuum limit (cf. [17], $N_f = 3$) the value of c_2 is not yet known exactly, but the sign probably remains the same and it is small. This would suggest then again the scaling, $c_4 \approx 10c_2$ case. We note, however, that our results are at the chiral limit, and therefore the lattice results may not follow this chiral scaling behavior.

In Ref. [29] it was shown that if the strength of the $U(1)$ anomaly, parameter C in the Lagrangian (4), is made μ_q-dependent, then the critical surface can have a nonmonotonic shape. Since C influences m_a, we can observe the same effect by considering the following dependence of m_a on μ_q, when solving (36):

$$\frac{m_a(\mu_q)}{m_\sigma} = 1 + \left(\frac{m_a(0)}{m_\sigma} - 1\right) e^{-\mu_q^2/\mu_{q,0}^2}. \tag{40}$$

For most of the curves with this chemical potential dependent anomaly parameter the results are very similar to what was obtained earlier; however, one can observe more exotic behavior, too, for some cases. For $\mu_{q,0}/m_\sigma = 0.17$ the result is shown in Fig. 6. Here the surface starts to bend

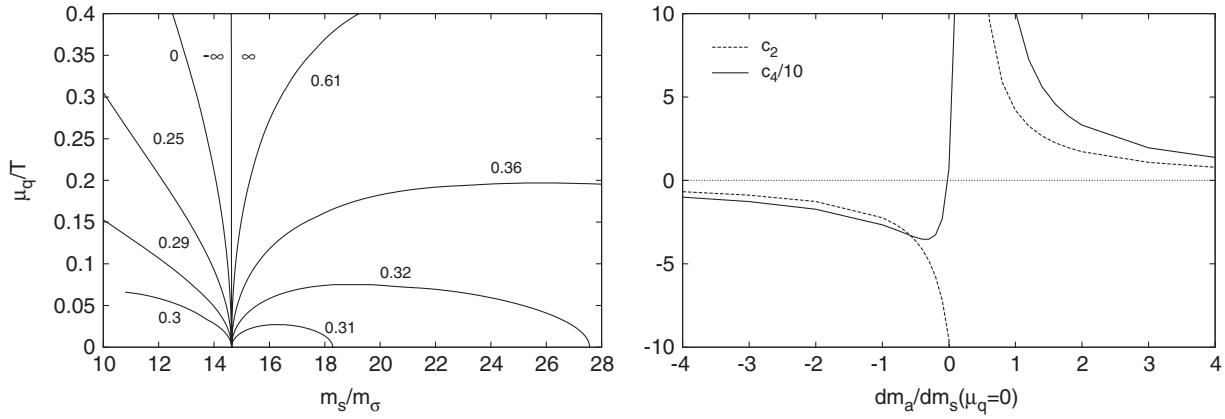

FIG. 5. Left panel: The m_s dependence of the critical μ_q/T obtained for $u = 10$ and $g^2 = 3$. The labels on the curves indicate the value of $dm_a/dm_s(\mu = 0)$. Right panel: The first two coefficients of the Taylor expansion in Eq. (39).

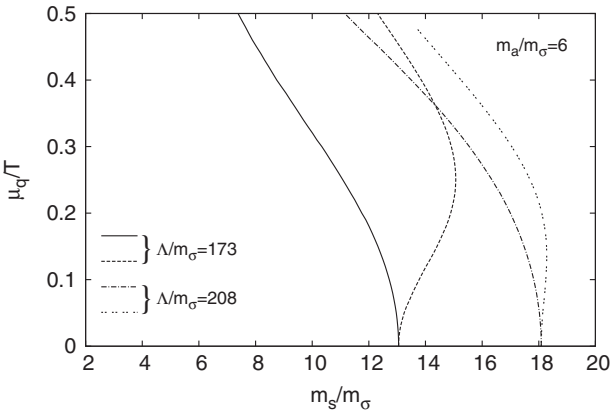

FIG. 6. Effect of a μ-dependent m_a on the m_s dependence of the critical μ_q/T obtained for $u = 10$. From the two pairs of lines having the same values of Λ/m_σ and m_a/m_σ, the one at the right is obtained by solving (36) with a μ-dependent m_a.

upwards, and later it turns back. This behavior can be very mild (as in our example with $\Lambda/m_\sigma = 208$). In this case the coarse lattice measurement would only detect the negative curvature; a high precision lattice measurement is necessary to reveal the positive curvature near $\mu_q = 0$. It is interesting that, considering the global behavior of the curve, the coarser lattice would give a more reliable result in this case.

VI. CONCLUSIONS

We discussed the behavior of the line of TCPs in the chiral limit ($m_{ud} = 0$) of the $U(3)_L \times U(3)_R$ quark model. We assumed that the value of the strange quark mass, where the TCP hits the $\mu_q \equiv 0$ line of the $m_s - \mu_q$ plane, is much larger than the critical temperature T_c. This is a good approximation in QCD, where the critical temperature is of order 160 MeV, while the constituent strange quark mass is about 450–500 MeV already at the physical point, and we expect that the second-order line reaches the chiral line ($m_{ud} = 0$) at much higher m_s masses. To estimate the value in the chiral limit we can use the results of [33,35], where the authors estimated $m_s^{\mathrm{TCP}} \approx 3$–$15 m_s^{\mathrm{phys}}$. Since we do not know exactly this value, we scanned a wide parameter range $m_s^{\mathrm{TCP}}(\mu_q = 0) \sim 2$–$50 m_\sigma$, where $m_s \gg T_c$ is fulfilled. We also assumed that the $\eta - a_0$ meson sector, which is heavier than the $\sigma - \pi$ sector because of the anomaly, is also much heavier than T_c. This is again plausible, since already at the physical point $m_a \sim 1$ GeV.

Under these circumstances the strange and the $\eta - a_0$ sector decouple from the point of view of the thermodynamics, which is completely determined by the light degrees of freedom, the $\sigma - \pi$ sector. This means that the nave one-loop perturbation theory would have an exponentially small sensitivity to the strange and anomaly scale. The only way the heavy sector can influence the thermodynamics is through the values of the parameters of the effective theory, i.e. when we include the renormalization group ideas into the analysis. We have to follow the running of the different parameters as well as the change in the degrees of freedom from the heavy scales down to the thermodynamic scale. This can be performed by following the RG flow with given degrees of freedom and determining the parameters of the effective theories by matching when the degrees of freedom change. The former yield logarithmic dependence on the heavy scale, and the latter effect is power-suppressed. Therefore in this work the RG flow is determined at one-loop level, and the matching is kept at tree level.

With the decoupling of the strange and $\eta - a_0$ meson sector, respectively, there are two stages of effective models in the $U(3)_L \times U(3)_R$ linear sigma model. The first is the $U(2)_L \times U(2)_R$, while the second is the $SU(2)_L \times SU(2)_R$ linear sigma model. We determined the corresponding beta functions in these models and solved the RG flow down to the scale of the temperature T. The thermodynamics is determined at one-loop level in [22]—we now included the running coupling constant in the result.

As a result we can determine the free energy for any given parameter sets, and we can determine the location of the TCP on the $\mu_q - T$ plane. With some plausible assumptions, the TCPs with fixed $\alpha = \mu_q/T$ (where μ_q is the quark chemical potential) form a surface in the $m_s - m_a - g^2$ space in the $U(3)_L \times U(3)_R$ linear sigma model. Surfaces for different α never cross; therefore the $\alpha = 0$ surface is a limiting surface.

If we want to draw consequences for QCD, we have to specify how m_a and g^2 depend on m_s in the chiral u, d regime. Since it is not known, we explored several possibilities. Depending on the details, this improved $SU(2) \times SU(2)$ linear sigma model can describe an upward bending (positive curvature) surface or a downward bending (negative curvature) surface. Taking into account the explicit chemical potential dependence of the anomaly constant, the curvature can change from positive to negative values along the curve. In this case the value of the curvature at $\mu_q = 0$ would yield false information about the global behavior of the curve.

We hope that future MC studies shed more light on the so far unknown dependencies of m_a and g^2 on m_s. Although it would be a hard task at the chiral limit, a qualitative understanding could be gained with a fixed m_{ud}, variable (but large) m_s measurement. If such information was provided, we could decide between the various scenarios described in this paper.

ACKNOWLEDGMENTS

The authors benefited from discussions with András Patkós and Péter Petreczky. This work is supported by the Hungarian Research Fund (OTKA) under Contracts No. T068108 and No. K77534.

APPENDIX A: RENORMALIZATION GROUP EQUATIONS IN THE $U(2)_L \times U(2)_R$ MODEL

We start from the renormalized Lagrangian of (20) and introduce the counterterm Lagrangian, which in Fourier space reads

$$\begin{aligned}\delta\mathcal{L}_{U(2)} &= \delta Z_\psi \bar\psi_2 \not{k} \psi_2 - \delta g \bar\psi_2(\varphi_5 - i\gamma_5 a_5)\psi_2 \\ &+ \frac{\delta Z}{2}\varphi(k^2 - \delta m_\varphi^2)\varphi + \frac{\delta Z}{2}a(k^2 - \delta m_a^2)a \\ &- \frac{\delta\lambda}{4}(\varphi^2 + a^2)^2 - \frac{\delta\lambda_2}{2}(\varphi^2 a^2 - (\varphi a)^2), \quad \text{(A1)}\end{aligned}$$

where we used the shorthand $\delta m^2_{\varphi/a} = \delta m^2 \mp \delta c$ and the observation that the wave function renormalization for the φ and a sector is the same.

The goal is to determine the counterterms at one-loop level. To this end we work at zero temperature in the symmetric phase. The method is to determine the expectation value of some physical observables and require finiteness. In order to simplify the treatment we introduce a background field for the σ field through the shift $\sigma \to \sigma + x$. The expansion in x is used for zero momentum external legs. The new Lagrangian obtained from (20) reads

$$\begin{aligned}\mathcal{L}_{U(2)} &= -\frac{m_\varphi^2}{2}x^2 - \frac{\lambda}{4}x^4 - \sigma x(m_\varphi^2 + \lambda x^2) + \bar\psi_2(i\partial\!\!\!/ - m_\psi)\psi_2 \\ &+ \frac{1}{2}(\partial_\mu\varphi)^2 + \frac{1}{2}(\partial_\mu a)^2 - \frac{m_\sigma^2}{2}\sigma^2 - \frac{m_\pi^2}{2}\pi_i^2 - \frac{m_\eta^2}{2}\eta^2 \\ &- \frac{m_A^2}{2}a_i^2 - g\bar\psi_2(\varphi_5 - i\gamma_5 a_5)\psi_2 - \lambda x\sigma(\varphi^2 + a^2) \\ &- \lambda_2 x\sigma a_i^2 - \lambda_2 x\eta\pi_i a_i - \frac{\lambda}{4}(\varphi^2 + a^2)^2 \\ &- \frac{\lambda_2}{2}[\varphi^2 a^2 - (\varphi a)^2], \quad \text{(A2)}\end{aligned}$$

where

$$\begin{aligned}&m_\psi = gx, \qquad m_\sigma^2 = m_\varphi^2 + 3\lambda x^2, \qquad m_\pi^2 = m_\varphi^2 + \lambda x^2, \\ &m_\eta^2 = m_a^2 + \lambda x^2, \qquad m_A^2 = m_a^2 + \lambda x^2 + \lambda_2 x^2, \quad \text{(A3)}\end{aligned}$$

with m_φ^2 and m_a^2 defined below (20).

1. The fermionic wave function and g renormalization

We calculate on the x background the fermion self-energy $\Sigma_\psi = i\langle \mathrm{T}\psi_2\bar\psi_2\rangle_{\mathrm{amp}}$. Introducing the notation $\int_p = \int\frac{d^4p}{(2\pi)^4}$ and using standard Feynman rules we find

$$\begin{aligned}\Sigma_\psi(k) &= -\delta Z_\psi \not{k} + x\delta g - ig^2\int_p [(iG_\sigma(p-k) \\ &+ 3iG_a(p-k))i\mathcal{G}(p) - (iG_\eta(p-k) \\ &+ 3iG_\pi(p-k))\gamma_5 i\mathcal{G}(p)\gamma_5], \quad \text{(A4)}\end{aligned}$$

where G and $\mathcal{G}$ are the bosonic and fermionic propagators defined as

$$G(p) = \frac{1}{p^2 - m^2 + i\varepsilon}, \qquad \mathcal{G}(p) = \frac{\not{p} + m}{p^2 - m^2 + i\varepsilon}, \quad \text{(A5)}$$

with the corresponding masses.

Since the integral has mass dimension, the parts proportional to $\not{k}$ or x are dimensionless, which means that they are at most logarithmically divergent. Therefore the masses should be taken into account only through a Taylor expansion. But the expansion in the bosonic masses yields $m^2 \sim x^2$ terms, which are convergent, so we can forget about the bosonic masses. The same is true for the fermionic mass in the denominator. What remains for the divergent piece is

$$\begin{aligned}\Sigma_\psi^{\mathrm{div}}(k) &= -\delta Z_\psi \not{k} + x\delta g + 4ig^2 \\ &\times \int_p G(p-k)[\mathcal{G}(p) - \gamma_5\mathcal{G}(p)\gamma_5]. \quad \text{(A6)}\end{aligned}$$

In the numerator we find $\not{p} + m - \gamma_5(\not{p} + m)\gamma_s = 2\not{p}$, which results in

$$\delta g = 0. \quad \text{(A7)}$$

For δZ_ψ we have to calculate the remaining integral. Doing this with standard techniques (cf., for example, [40]) using cutoff regularization we find

$$\Sigma_\psi^{\mathrm{div}}(k) = \left(-\delta Z_\psi - \frac{g^2}{4\pi^2}\ln\frac{\Lambda^2}{\mu^2}\right)\not{k}, \quad \text{(A8)}$$

and so, the counterterm ensuring the finiteness of $\Sigma_\psi(k)$ is

$$\delta Z_\psi = -\frac{g^2}{4\pi^2}\ln\frac{\Lambda^2}{\mu^2}. \quad \text{(A9)}$$

2. The bosonic wave function and λ renormalization

We calculate next the σ self-energy on the given x background. We find

$$\begin{aligned}\Sigma_\sigma(k) &= -\delta Z k^2 + \delta m_\varphi^2 + 3\delta\lambda x^2 + 3\lambda\int_p iG_\sigma(p) + 3\lambda\int_p iG_\pi(p) + \lambda\int_p iG_\eta(p) + 3(\lambda+\lambda_2)\int_p iG_a(p) \\ &- ig^2\int_p \mathrm{Tr}[\mathcal{G}(p-k)\mathcal{G}(p)] + 18i\lambda^2x^2\int_p G_\sigma(p-k)G_\sigma(p) + 6i\lambda^2x^2\int_p G_\pi(p-k)G_\pi(p) \\ &+ 2i\lambda^2x^2\int_p G_\eta(p-k)G_\eta(p) + 6i(\lambda+\lambda_2)^2x^2\int_p G_a(p-k)G_a(p). \quad \text{(A10)}\end{aligned}$$

The minus sign is because the fermionic bubble involves a closed fermion loop. To determine δZ and δm_φ we need only the $x = 0$ sector:

$$\Sigma_\sigma(k, x = 0) = -\delta Z k^2 + \delta m_\varphi^2 + 6\lambda \int_p iG_\varphi(p) + (4\lambda + 3\lambda_2) \int_p iG_a(p) - ig^2 \int_p \mathrm{Tr}[\mathcal{G}(p - k)\mathcal{G}(p)]. \quad \text{(A11)}$$

After evaluating the integrals, without writing the Λ^2 corrections we find

$$\Sigma_\sigma^{\mathrm{div}}(k, x = 0) = -\delta Z k^2 + \delta m_\varphi^2 + \frac{6\lambda}{16\pi^2} m_\varphi^2 \ln\frac{m_\varphi^2}{\Lambda^2} + \frac{4\lambda + 3\lambda_2}{16\pi^2} m_a^2 \ln\frac{m_a^2}{\Lambda^2} - \frac{g^2}{24\pi^2} k^2 \ln\frac{k^2}{\Lambda^2}. \quad \text{(A12)}$$

Therefore

$$\delta Z = \frac{g^2}{12\pi^2} \ln\frac{\Lambda^2}{\mu^2}, \qquad \delta m_\varphi^2 = \frac{1}{16\pi^2} \ln\frac{\Lambda^2}{\mu^2}[6\lambda m_\varphi^2 + (4\lambda + 3\lambda_2) m_a^2]. \quad \text{(A13)}$$

For the determination of $\delta\lambda$ we need the self-energy at $k = 0$. After evaluating the integrals we find

$$\Sigma_\sigma^{\mathrm{div}}(k = 0) = \delta m_\varphi^2 - \frac{1}{16\pi^2} \ln\frac{\Lambda^2}{\mu^2}[6\lambda m_\varphi^2 + (4\lambda + 3\lambda_2) m_a^2] + 3\delta\lambda x^2 - \frac{3x^2}{16\pi^2} \ln\frac{\Lambda^2}{\mu^2}[13\lambda^2 + 3(\lambda + \lambda_2)^2 - 4g^4]. \quad \text{(A14)}$$

We obtain for δm_φ^2 the previous result given in (A13), and we also have

$$\delta\lambda = \frac{1}{16\pi^2} \ln\frac{\Lambda^2}{\mu^2}[13\lambda^2 + 3(\lambda + \lambda_2)^2 - 4g^4]. \quad \text{(A15)}$$

3. Renormalization of λ_2

We apply the procedure above, but now for the a self-energy. Since the wave function renormalization is the same as for φ, we need only the $k = 0$ case. We find

$$\Sigma_a(k = 0) = \delta m_a^2 + (\delta\lambda + \delta\lambda_2)x^2 + 5\lambda \int_p iG_a(p) + (3\lambda + 2\lambda_2) \int_p iG_\pi(p) + \lambda \int_p iG_\eta(p) + (\lambda + \lambda_2) \int_p iG_\sigma(p) - ig^2 \int_p \mathrm{Tr}[\mathcal{G}(p)\mathcal{G}(p)] + 4i(\lambda + \lambda_2)^2 x^2 \int_p G_\sigma(p) G_a(p) + i\lambda_2^2 x^2 \int_p G_\pi(p) G_\eta(p). \quad \text{(A16)}$$

After evaluating the integrals we find for the divergent pieces

$$\Sigma_a^{\mathrm{div}}(k = 0) = \delta m_a^2 + (\delta\lambda + \delta\lambda_2)x^2 - \frac{1}{16\pi^2} \ln\frac{\Lambda^2}{\mu^2}[6\lambda m_a^2 + (4\lambda + 3\lambda_2) m_\varphi^2] - \frac{x^2}{16\pi^2} \ln\frac{\Lambda^2}{\mu^2}[16\lambda^2 + 18\lambda\lambda_2 + 5\lambda_2^2 - 12g^4]. \quad \text{(A17)}$$

For the a-mass counterterm we find the following expression:

$$\delta m_a^2 = \frac{1}{16\pi^2} \ln\frac{\Lambda^2}{\mu^2}[6\lambda m_a^2 + (4\lambda + 3\lambda_2) m_\varphi^2], \quad \text{(A18)}$$

which is the same as the expression for the σ mass, with the $m_\varphi \leftrightarrow m_a$ interchange. This shows that the sum and the difference of the masses are renormalized multiplicatively. Since $m_{\varphi/a}^2 = m^2 \mp c$, so we find

$$\delta c = c \frac{2\lambda - 3\lambda_2}{16\pi^2} \ln\frac{\Lambda^2}{\mu^2}, \qquad \delta m^2 = m^2 \frac{10\lambda + 3\lambda_2}{16\pi^2} \ln\frac{\Lambda^2}{\mu^2}. \quad \text{(A19)}$$

From (A17) we can also read off the counterterm for $\lambda + \lambda_2$:

$$\delta\lambda + \delta\lambda_2 = \frac{1}{16\pi^2} \ln\frac{\Lambda^2}{\mu^2}[16\lambda^2 + 18\lambda\lambda_2 + 5\lambda_2^2 - 12g^4]. \quad \text{(A20)}$$

Comparing it with the expression of $\delta\lambda$ given in (A15) we find

$$\delta\lambda_2 = \frac{2}{16\pi^2} \ln\frac{\Lambda^2}{\mu^2}[\lambda_2(6\lambda + \lambda_2) - 4g^4]. \quad \text{(A21)}$$

4. β functions

The bare-field Lagrangian reads

$$\mathcal{L}_{U(2),0} = \bar\psi_{02}[i\partial - g_0(\varphi_{05} - i\gamma_5 a_{05})]\psi_{02} + \frac{1}{2}(\partial_\mu\varphi_0)^2 + \frac{1}{2}(\partial_\mu a_0)^2 - \frac{m_{0\varphi}^2}{2}\varphi_0^2 - \frac{m_{0a}^2}{2}a_0^2 - \frac{\lambda_0}{4}(\varphi_0^2 + a_0^2)^2 - \frac{\lambda_{02}}{2}[\varphi_0^2 a_0^2 - (\varphi_0 a_0)^2], \quad \text{(A22)}$$

where all the fields and couplings are bare. The bare couplings are RG invariant, since they depend only on the regularization:

$$\frac{dg_0}{d\ln\mu} = \frac{dm_{0\varphi}^2}{d\ln\mu} = \frac{dm_{0a}^2}{d\ln\mu} = \frac{d\lambda_0}{d\ln\mu} = \frac{d\lambda_{02}}{d\ln\mu} = 0, \quad \text{(A23)}$$

where

$$\frac{d}{d\ln\mu} = \frac{\partial}{\partial\ln\mu} + \beta_g\frac{\partial}{\partial g} + \beta_\lambda\frac{\partial}{\partial\lambda} + \beta_2\frac{\partial}{\partial\lambda_2} + \gamma_\varphi\frac{\partial}{\partial m_\varphi^2} + \gamma_a\frac{\partial}{\partial m_a^2}. \tag{A24}$$

To obtain the bare quantities from the counterterms, we first have to change to renormalized fields $\psi_{02} = Z_\psi^{1/2}\psi_2$, $\varphi_0 = Z^{1/2}\varphi$, and $a_0 = Z^{1/2}a$:

$$\begin{aligned}\mathcal{L}_2 = {}& \bar\psi_2[Z_\psi i\partial\!\!\!/ - Z_\psi Z^{1/2} g_0(\varphi_5 - i\gamma_5 a_5)]\psi_2 \\ & + \frac{Z}{2}(\partial_\mu\varphi)^2 + \frac{Z}{2}(\partial_\mu a)^2 - \frac{Zm_{0\varphi}^2}{2}\varphi^2 - \frac{Zm_{0a}^2}{2}a^2 \\ & - \frac{Z^2\lambda_0}{4}(\varphi^2 + a^2)^2 - \frac{Z^2\lambda_{02}}{2}[\varphi^2 a^2 - (\varphi a)^2].\end{aligned} \tag{A25}$$

Comparing it with the renormalized Lagrangian defined as the sum of (20) and (A1) we find $Z_\psi = 1 + \delta Z_\psi$ and $Z = 1 + \delta Z$, so that the relations between the bare couplings and counterterms read

$$\begin{aligned} Z_\psi Z^{1/2} g_0 &= g + \delta g, \qquad Zm_{0\varphi}^2 = m_\varphi^2 + \delta m_\varphi^2, \\ Zm_{0a}^2 &= m_a^2 + \delta m_a^2, \qquad Z^2\lambda_0 = \lambda + \delta\lambda, \\ Z^2\lambda_{02} &= \lambda_2 + \delta\lambda_2. \end{aligned} \tag{A26}$$

These relations can be inverted, and at one-loop level we obtain

$$\begin{aligned} g_0 &= g - (\tfrac{1}{2}\delta Z + \delta Z_\psi)g + \delta g, \\ m_{0\varphi}^2 &= m_\varphi^2 - \delta Z m_\varphi^2 + \delta m_\varphi^2, \\ m_{0a}^2 &= m_a^2 - \delta Z m_a^2 + \delta m_a^2, \\ \lambda_0 &= \lambda - 2\delta Z\lambda + \delta\lambda, \\ \lambda_{02} &= \lambda_2 - 2\delta Z\lambda_2 + \delta\lambda_2. \end{aligned} \tag{A27}$$

Perturbative hierarchy requires that when there is a $\ln\mu$ dependence in the quantity, then only the $\partial/(\partial\ln\mu)$ derivative acts on it. Then, using (A24) we find

$$\frac{dg_0}{d\ln\mu} = \beta_g - \frac{\partial}{\partial\ln\mu}\left[\left(\frac{1}{2}\delta Z + \delta Z_\psi\right)g - \delta g\right] = 0, \tag{A28}$$

and in consequence

$$\beta_g = \frac{\partial}{\partial\ln\mu}\left[\left(\frac{1}{2}\delta Z + \delta Z_\psi\right)g - \delta g\right]. \tag{A29}$$

In a similar way we find

$$\begin{aligned} \gamma_\varphi &= \frac{\partial}{\partial\ln\mu}[\delta Z m_\varphi^2 - \delta m_\varphi^2], \\ \gamma_a &= \frac{\partial}{\partial\ln\mu}[\delta Z m_a^2 - \delta m_a^2], \\ \beta_\lambda &= \frac{\partial}{\partial\ln\mu}[2\delta Z\lambda - \delta\lambda], \\ \beta_2 &= \frac{\partial}{\partial\ln\mu}[2\delta Z\lambda_2 - \delta\lambda_2]. \end{aligned} \tag{A30}$$

Using the expression of the counterterms determined in previous subsections of this sections we have

$$\begin{aligned} \frac{\partial\delta Z_\psi}{\partial\ln\mu} &= \frac{g^2}{2\pi^2}, \\ \frac{\partial\delta Z}{\partial\ln\mu} &= -\frac{g^2}{6\pi^2}, \\ \frac{\partial\delta g}{\partial\ln\mu} &= 0, \\ \frac{\partial\delta\lambda}{\partial\ln\mu} &= -\frac{1}{8\pi^2}[13\lambda^2 + 3(\lambda+\lambda_2)^2 - 4g^4], \\ \frac{\partial\delta\lambda_2}{\partial\ln\mu} &= -\frac{1}{4\pi^2}[\lambda_2(6\lambda+\lambda_2) - 4g^4], \\ \frac{\partial\delta m_{\varphi/a}^2}{\partial\ln\mu} &= -\frac{1}{8\pi^2}[6\lambda m_{\varphi/a}^2 + (4\lambda+3\lambda_2)m_{a/\varphi}^2]. \end{aligned} \tag{A31}$$

With these expressions, we obtain from (A29) and (A30) the following one-loop β functions:

$$\frac{dg}{d\ln\mu} = \beta_g = \frac{5g^3}{12\pi^2}, \tag{A32a}$$

$$\frac{d\lambda}{d\ln\mu} = \beta_\lambda = \frac{1}{8\pi^2}\left[13\lambda^2 + 3(\lambda+\lambda_2)^2 - 4g^4 - \frac{8}{3}g^2\lambda\right], \tag{A32b}$$

$$\frac{d\lambda_2}{d\ln\mu} = \beta_2 = \frac{1}{4\pi^2}\left[\lambda_2(6\lambda+\lambda_2) - 4g^4 - \frac{4}{3}g^2\lambda_2\right], \tag{A32c}$$

$$\frac{dm_{\varphi/a}^2}{d\ln\mu} = \gamma_{\varphi/a} = \frac{1}{8\pi^2}\left[\left(6\lambda - \frac{4}{3}g^2\right)m_{\varphi/a}^2 + (4\lambda+3\lambda_2)m_{a/\varphi}^2\right]. \tag{A32d}$$

APPENDIX B: RENORMALIZATION GROUP IN THE $SU(2)_L \times SU(2)_R$ LINEAR SIGMA MODEL

We start from the renormalized Lagrangian (26) and add to it the following counterterm Lagrangian:

$$\begin{aligned}\delta\mathcal{L}_{SU(2)} = {}& \bar\psi[Z_\psi i\partial\!\!\!/ - \delta g(\sigma + i\tau_i\pi_i)]\psi + \frac{Z}{2}(\partial_\mu\varphi)^2 \\ & - \frac{\delta m_\varphi^2}{2}\varphi^2 - \frac{\delta\lambda}{4}(\sigma^2 + \pi_i^2)^2.\end{aligned} \tag{B1}$$

The goal is to determine the counterterms at one-loop level. To do this, we will follow the same strategy as in Appendix A. To facilitate the discussion we introduce again the background field x. After the shift $\sigma \to \sigma + x$ the Lagrangian reads

$$\mathcal{L}_{SU(2)} = -\frac{m_\varphi^2}{2}x^2 - \frac{\lambda}{4}x^2 - \sigma x(m_\varphi^2 + \lambda x^2) + \bar{\psi}(i\partial - m_\psi)\psi - g\bar{\psi}(\sigma + i\tau_i\pi_i)\psi + \frac{1}{2}(\partial_\mu\sigma)^2 - \frac{m_\sigma^2}{2}\sigma^2 + \frac{1}{2}(\partial_\mu\pi)^2 - \frac{m_\pi^2}{2}\pi^2 - \lambda x\sigma(\sigma^2 + \pi_i^2) - \frac{\lambda}{4}(\sigma^2 + \pi_i^2)^2, \quad \text{(B2)}$$

where

$$m_\psi^2 = gx, \qquad m_\sigma^2 = m_\varphi^2 + 3\lambda x^2, \qquad m_\pi^2 = m_\varphi^2 + \lambda x^2. \quad \text{(B3)}$$

1. The fermion wave function and g renormalization

We calculate the fermion self-energy on the background x:

$$\Sigma_\psi(k, x) = -\delta Z_\psi \not{k} + \delta g x - ig^2\int_p [iG_\sigma(p-k)i\mathcal{G}(p) - 3iG_\pi(p-k)\gamma_5 i\mathcal{G}(p)\gamma_5], \quad \text{(B4)}$$

where G_σ, G_π, and $\mathcal{G}$ are the bosonic and fermion propagators introduced in (A5) with the corresponding masses given in (B3). Taylor expanding the bosonic propagators in x and using that γ_5 anticommutes with all the other gamma matrices, we find

$$\Sigma_\psi(k) = \delta g x - \delta Z_\psi \not{k} + 2ig^2\int_p \frac{2\not{p} - m_\psi}{((p-k)^2 - m_\varphi^2 + i\varepsilon)(p^2 - m_\psi^2 + i\varepsilon)}. \quad \text{(B5)}$$

After evaluating the integrals, finiteness of the result requires the following expressions for the counterterms:

$$\delta Z_\psi = -\frac{g^2}{8\pi^2}\ln\frac{\Lambda^2}{\mu^2}, \qquad \delta g = -\frac{g^3}{8\pi^2}\ln\frac{\Lambda^2}{\mu^2}. \quad \text{(B6)}$$

2. The σ mass, wave function, and λ renormalization

Next, we calculate the σ self-energy:

$$\Sigma_\sigma(k) = -\delta Z k^2 + \delta m_\varphi^2 + 3\delta\lambda x^2 + 3\lambda\int_p iG_\sigma(p) + 3\lambda\int_p iG_\pi(p) - ig^2\int_p \mathrm{Tr}[\mathcal{G}(p-k)\mathcal{G}(p)] + 18i\lambda^2x^2\int_p G_\sigma(p-k)G_\sigma(p) + 6i\lambda^2x^2\int_p G_\pi(p-k)G_\pi(p). \quad \text{(B7)}$$

The minus sign is because of the fermionic bubble. After evaluating the integrals we find, neglecting the Λ^2 corrections

$$\Sigma_\sigma^{\mathrm{div}}(k) = -\delta Z k^2 + \delta m_\varphi^2 + 3\delta\lambda x^2 - \frac{3\lambda}{16\pi^2}(2m_\varphi^2 + 4\lambda x^2)\times\ln\frac{\Lambda^2}{\mu^2} + \frac{g^2}{4\pi^2}\left(\frac{k^2}{6} + 3g^2x^2\right)\ln\frac{\Lambda^2}{\mu^2} - \frac{3\lambda^2}{2\pi^2}\ln\frac{\Lambda^2}{\mu^2}. \quad \text{(B8)}$$

Therefore, the expression of the counterterms is

$$\delta Z = \frac{g^2}{24\pi^2}\ln\frac{\Lambda^2}{\mu^2}, \qquad \delta m_\varphi^2 = \frac{3\lambda}{8\pi^2}m_\varphi^2\ln\frac{\Lambda^2}{\mu^2}, \qquad \delta\lambda = \frac{3\lambda^2 - g^4}{4\pi^2}\ln\frac{\Lambda^2}{\mu^2}. \quad \text{(B9)}$$

3. β functions

We again use the fact that the bare couplings are renormalization group invariant:

$$\frac{dg_0}{d\ln\mu} = \frac{dm_0^2}{d\ln\mu} = \frac{d\lambda_0}{d\ln\mu} = 0, \quad \text{(B10)}$$

where

$$\frac{d}{d\ln\mu} = \frac{\partial}{\partial\ln\mu} + \beta_g\frac{\partial}{\partial g} + \beta_\lambda\frac{\partial}{\partial\lambda} + \gamma_\varphi\frac{\partial}{\partial m_\varphi^2}. \quad \text{(B11)}$$

This leads to

$$\beta_g = \frac{\partial}{\partial\ln\mu}\left[\left(\delta Z + \frac{1}{2}\delta Z_\psi\right)g - \delta g\right], \qquad \gamma = \frac{\partial}{\partial\ln\mu}[\delta Z m_\varphi^2 - \delta m_\varphi^2], \qquad \beta_\lambda = \frac{\partial}{\partial\ln\mu}[2\delta Z\lambda - \delta\lambda]. \quad \text{(B12)}$$

Using the counterterms determined in the previous two subsections one has

$$\frac{\partial\delta Z_\psi}{\partial\ln\mu} = \frac{g^2}{4\pi^2}, \qquad \frac{\partial\delta Z}{\partial\ln\mu} = -\frac{g^2}{12\pi^2}, \qquad \frac{\partial\delta g}{\partial\ln\mu} = \frac{g^3}{4\pi^2}, \qquad \frac{\partial\delta\lambda}{\partial\ln\mu} = \frac{-3\lambda^2 + g^4}{2\pi^2}, \qquad \frac{\partial\delta m_\varphi^2}{\partial\ln\mu} = -\frac{3\lambda m_\varphi^2}{4\pi^2}. \quad \text{(B13)}$$

Then, we find the following one-loop β functions:

$$\frac{dg}{d\ln\mu} = \beta_g = -\frac{5g^3}{24\pi^2},$$
$$\frac{d\lambda}{d\ln\mu} = \beta_\lambda = \frac{9\lambda^2 - 3g^4 - \lambda g^2}{6\pi^2}, \tag{B14}$$
$$\frac{1}{m_\varphi^2}\frac{dm_\varphi^2}{d\ln\mu} = \gamma = \frac{9\lambda - g^2}{12\pi^2}m_\varphi^2.$$

APPENDIX C: NUMERICAL STRATEGY TO SOLVE THE TCP EQUATIONS

For numerical purposes it is advantageous to choose α, $g^2 = g^2(\mu)$, and m_a as parametrization variables. Then we can proceed as follows. From (36) we find

$$u(\mu) = \frac{6\bar{\mathcal{F}}(\alpha)}{\pi^2}g^2, \qquad T^2 = \frac{1}{2g^2[\frac{g^2\bar{\mathcal{F}}(\alpha)}{\pi^2} + 1 + \frac{3}{\pi^2}\alpha^2]}, \tag{C1}$$

and then from (27)

$$\Lambda_0^2 = \mu^2 e^{-(24\pi^2/5g^2(\mu))} = \frac{e^{2\xi-(24\pi^2/5g^2(\mu))}}{2g^2(\mu)[\frac{g^2(\mu)\bar{\mathcal{F}}(\alpha)}{\pi^2} + 1 + \frac{3}{\pi^2}\alpha^2]}. \tag{C2}$$

Once we know $g^2(\mu)$, T, Λ_0, and $u(\mu)$ we can compute m_σ by solving $m_\sigma^2 = m_\sigma^2(\mu = m_\sigma)$ using (33). Since now $m_\sigma(\mu) = 1$ is the mass scale, in view of (33) we have to solve

$$m_\sigma = \exp\left[\frac{7g_0^2}{24\pi^2}\int_0^{\ln m_\sigma/\mu}\frac{ds}{1 + bg^2(\mu)s}\frac{1 + 6Yz(s)}{1 - 3Yz(s)}\right], \tag{C3}$$

where $Y = (u(\mu) - 1)/(3u(\mu) + 4)$. If we know m_σ, then we can have $g^2(m_\sigma)$ from (27) which can be kept fixed.

From the running of g (27) and u (31) we find

$$g^2(m_a) = \frac{g^2}{1 + \frac{5g^2}{12\pi^2}\ln\frac{m_a}{\mu}},$$
$$\frac{2u(m_a) - 1}{3u(m_a) + 4} = \frac{2u(\mu) - 1}{3u(\mu) + 4}\left(1 + \frac{\ln(m_a/\mu)}{\ln(\mu/\Lambda_0)}\right)^{21/5}. \tag{C4}$$

From (28) we find

$$\bar{\Lambda}_0^4 = 2m_a^6 g^2(\mu)\left[\frac{g^2(\mu)\bar{\mathcal{F}}(\alpha)}{\pi^2} + 1 + \frac{3}{\pi^2}\alpha^2\right]e^{24\pi^2/5g^2(\mu)}. \tag{C5}$$

Having $\bar{\Lambda}_0^4$, $u(m_a)$, and $u(m_s)$ we can use the solution of the $U(2)_L \times U(2)_R$ RG running (25) to find m_s. Finally from m_s and $g(m_a)$ we compute from (21):

$$g^2(m_s) = \frac{g^2(m_a)}{1 - \frac{5g^2}{6\pi^2}\ln\frac{m_s}{m_a}}. \tag{C6}$$

[1] P. de Forcrand, Proc. Sci., LAT2009 (2009) 010 [arXiv:1005.0539].
[2] Z. Fodor and S. D. Katz, arXiv:0908.3341.
[3] K. Fukushima and T. Hatsuda, Rep. Prog. Phys. **74**, 014001 (2011).
[4] O. Philipsen, arXiv:1009.4089.
[5] Z. Fodor and S. D. Katz, J. High Energy Phys. 04 (2004) 050.
[6] F. Csikor, G. I. Egri, Z. Fodor, S. D. Katz, K. K. Szabó, and A. I. Toth, J. High Energy Phys. 05 (2004) 046.
[7] S. Ejiri, C. R. Allton, S. J. Hands, O. Kaczmarek, F. Karsch, E. Laermann, and C. Schmidt, Prog. Theor. Phys. Suppl. **153**, 118 (2004).
[8] A. Li, Proc. Sci., LAT2009 (2009) 011 [arXiv:1002.4459].
[9] S. Ejiri, T. Hatsuda, N. Ishii, Y. Maezawa, N. Ukita, S. Aoki, and K. Kanaya, Proc. Sci., LAT2006 (2006) 132 [arXiv:hep-lat/0609075].
[10] R. V. Gavai and S. Gupta, Phys. Rev. D **78**, 114503 (2008).
[11] C. R. Allton *et al.*, Phys. Rev. D **71**, 054508 (2005).
[12] P. de Forcrand and O. Philipsen, J. High Energy Phys. 11 (2008) 012.
[13] P. de Forcrand and O. Philipsen, Proc. Sci., LAT2008 (2008) 208 [arXiv:0811.3858].
[14] P. de Forcrand and O. Philipsen, J. High Energy Phys. 01 (2007) 077.
[15] P. de Forcrand, S. Kim, and O. Philipsen, Proc. Sci., LAT2007 (2007) 178 [arXiv:0711.0262].
[16] J. T. Mościcki, M. Wos, M. Lamanna, P. de Forcrand, and O. Philipsen, Comput. Phys. Commun. **181**, 1715 (2010).
[17] O. Philipsen, Nucl. Phys. **A830**, 713C (2009).
[18] P. de Forcrand and O. Philipsen, Phys. Rev. Lett. **105**, 152001 (2010).
[19] R. Casalbuoni, Proc. Sci., CPOD2006 (2006) 001 [arXiv:hep-ph/0610179].
[20] J. Berges and K. Rajagopal, Nucl. Phys. **B538**, 215 (1999).
[21] O. Scavenius, A. Mocsy, I. N. Mishustin, and D. H. Rischke, Phys. Rev. C **64**, 045202 (2001).
[22] A. Jakovác, A. Patkós, Zs. Szép, and P. Szépfalusy, Phys. Lett. B **582**, 179 (2004).
[23] E. S. Bowman and J. I. Kapusta, Phys. Rev. C **79**, 015202 (2009).
[24] P. Kovács and Zs. Szép, Phys. Rev. D **75**, 025015 (2007).
[25] P. Kovács and Zs. Szép, Phys. Rev. D **77**, 065016 (2008).

[26] B. J. Schaefer and M. Wagner, Phys. Rev. D **79**, 014018 (2009).
[27] K. Fukushima, Phys. Rev. D **77**, 114028 (2008); **78**, 039902(E) (2008).
[28] K. Fukushima, Phys. Rev. D **78**, 114019 (2008).
[29] J. W. Chen, K. Fukushima, H. Kohyama, K. Ohnishi, and U. Raha, Phys. Rev. D **80**, 054012 (2009).
[30] S. Gupta, arXiv:0712.0434.
[31] S. Gupta, J. Phys. G **35**, 104018 (2008).
[32] J. T. Lenaghan, D. H. Rischke, and J. Schaffner-Bielich, Phys. Rev. D **62**, 085008 (2000).
[33] T. Herpay and Zs. Szép, Phys. Rev. D **74**, 025008 (2006).
[34] V. B. Jovanović, S. R. Ignjatović, D. Borka, and P. Jovanović, arXiv:1011.1749.
[35] O. Philipsen, Proc. Sci., LAT2005 (2006) 016 [arXiv:hep-lat/0510077].
[36] J. Collins, *Renormalization*, Cambridge Monographs for Mathematical Physics (Cambridge University Press, Cambridge, England, 1984).
[37] K. Kajantie, M. Laine, K. Rummukainen, and M. E. Shaposhnikov, Nucl. Phys. **B458**, 90 (1996).
[38] G. 't Hooft, Phys. Rev. D **14**, 3432 (1976); **18**, 2199(E) (1978).
[39] G. 't Hooft, Phys. Rev. Lett. **37**, 8 (1976).
[40] M. E. Peskin and D. V. Schroeder, *An Introduction to Quantum Field Theory* (Westview, New York, 1995).